



Designation: **E1921–14** **E1921 – 14a**

## Standard Test Method for Determination of Reference Temperature, $T_o$ , for Ferritic Steels in the Transition Range<sup>1</sup>

This standard is issued under the fixed designation E1921; the number immediately following the designation indicates the year of original adoption or, in the case of revision, the year of last revision. A number in parentheses indicates the year of last reappraisal. A superscript epsilon ( $\epsilon$ ) indicates an editorial change since the last revision or reappraisal.

### 1. Scope

1.1 This test method covers the determination of a reference temperature,  $T_o$ , which characterizes the fracture toughness of ferritic steels that experience onset of cleavage cracking at elastic, or elastic-plastic  $K_{Jc}$  instabilities, or both. The specific types of ferritic steels (**3.2.1**) covered are those with yield strengths ranging from 275 to 825 MPa (40 to 120 ksi) and weld metals, after stress-relief annealing, that have 10 % or less strength mismatch relative to that of the base metal.

1.2 The specimens covered are fatigue precracked single-edge notched bend bars, SE(B), and standard or disk-shaped compact tension specimens, C(T) or DC(T). A range of specimen sizes with proportional dimensions is recommended. The dimension on which the proportionality is based is specimen thickness.

1.3 Median  $K_{Jc}$  values tend to vary with the specimen type at a given test temperature, presumably due to constraint differences among the allowable test specimens in 1.2. The degree of  $K_{Jc}$  variability among specimen types is analytically predicted to be a function of the material flow properties (**1**)<sup>2</sup> and decreases with increasing strain hardening capacity for a given yield strength material. This  $K_{Jc}$  dependency ultimately leads to discrepancies in calculated  $T_o$  values as a function of specimen type for the same material.  $T_o$  values obtained from C(T) specimens are expected to be higher than  $T_o$  values obtained from SE(B) specimens. Best estimate comparisons of several materials indicate that the average difference between C(T) and SE(B)-derived  $T_o$  values is approximately 10°C (**2**). C(T) and SE(B)  $T_o$  differences up to 15°C have also been recorded (**3**). However, comparisons of individual, small datasets may not necessarily reveal this average trend. Datasets which contain both C(T) and SE(B) specimens may generate  $T_o$  results which fall between the  $T_o$  values calculated using solely C(T) or SE(B) specimens. It is therefore strongly recommended that the specimen type be reported along with the derived  $T_o$  value in all reporting, analysis, and discussion of results. This recommended reporting is in addition to the requirements in 11.1.1.

1.4 Requirements are set on specimen size and the number of replicate tests that are needed to establish acceptable characterization of  $K_{Jc}$  data populations.

1.5  $T_o$  is dependent on loading rate.  $T_o$  is evaluated for a quasi-static loading rate range with  $0.1 < dK/dt < 2$  MPa $\sqrt{m/s}$ . Slowly loaded specimens ( $dK/dt < 0.1$  MPa $\sqrt{m/s}$ ) can be analyzed if environmental effects are known to be negligible. Provision is also made for higher loading rates ( $dK/dt > 2$  MPa $\sqrt{m/s}$ ).

1.6 The statistical effects of specimen size on  $K_{Jc}$  in the transition range are treated using weakest-link theory (**4**) applied to a three-parameter Weibull distribution of fracture toughness values. A limit on  $K_{Jc}$  values, relative to the specimen size, is specified to ensure high constraint conditions along the crack front at fracture. For some materials, particularly those with low strain hardening, this limit may not be sufficient to ensure that a single-parameter ( $K_{Jc}$ ) adequately describes the crack-front deformation state (**5**).

1.7 Statistical methods are employed to predict the transition toughness curve and specified tolerance bounds for 1T specimens of the material tested. The standard deviation of the data distribution is a function of Weibull slope and median  $K_{Jc}$ . The procedure for applying this information to the establishment of transition temperature shift determinations and the establishment of tolerance limits is prescribed.

1.8 This test method assumes that the test material is macroscopically homogeneous such that the materials have uniform tensile and toughness properties. The fracture toughness evaluation of nonuniform materials is not amenable to the statistical analysis methods employed in the main body of this test method. Application of the analysis of this test method to an inhomogeneous

<sup>1</sup> This test method is under the jurisdiction of ASTM Committee E08 on Fatigue and Fracture and is the direct responsibility of E08.07 on Fracture Mechanics. Current edition approved Aug. 1, 2014 Dec. 15, 2014. Published January 2015. Originally approved in 1997. Last previous edition approved in 2013 as E1921–13a. E1921 – 14. DOI: 10.1520/E1921-14.10.1520/E1921-14A.

<sup>2</sup> The boldface numbers in parentheses refer to the list of references at the end of this standard.

material will result in an inaccurate estimate of the transition reference value  $T_o$  and non-conservative confidence bounds. For example, multipass weldments can create heat-affected and brittle zones with localized properties that are quite different from either the bulk material or weld. Thick section steel also often exhibits some variation in properties near the surfaces. Metallography and initial screening may be necessary to verify the applicability of these and similarly graded materials. An appendix to analyze the cleavage toughness properties of nonuniform or inhomogeneous materials is currently being prepared. In the interim, users are referred to (6-8) for procedures to analyze inhomogeneous materials.

1.9 *This standard does not purport to address all of the safety concerns, if any, associated with its use. It is the responsibility of the user of this standard to establish appropriate safety and health practices and determine the applicability of regulatory limitations prior to use.*

## 2. Referenced Documents

### 2.1 ASTM Standards:<sup>3</sup>

E4 Practices for Force Verification of Testing Machines

E8/E8M Test Methods for Tension Testing of Metallic Materials

E23 Test Methods for Notched Bar Impact Testing of Metallic Materials

E74 Practice of Calibration of Force-Measuring Instruments for Verifying the Force Indication of Testing Machines

E111 Test Method for Young's Modulus, Tangent Modulus, and Chord Modulus

E177 Practice for Use of the Terms Precision and Bias in ASTM Test Methods

E208 Test Method for Conducting Drop-Weight Test to Determine Nil-Ductility Transition Temperature of Ferritic Steels

E399 Test Method for Linear-Elastic Plane-Strain Fracture Toughness  $K_{Ic}$  of Metallic Materials

E436 Test Method for Drop-Weight Tear Tests of Ferritic Steels

E561 Test Method for  $K-R$  Curve Determination

E691 Practice for Conducting an Interlaboratory Study to Determine the Precision of a Test Method

E1820 Test Method for Measurement of Fracture Toughness

E1823 Terminology Relating to Fatigue and Fracture Testing

## 3. Terminology

3.1 Terminology given in Terminology E1823 is applicable to this test method.

### 3.2 Definitions:

3.2.1 *ferritic steels*—are typically carbon, low-alloy, and higher alloy grades. Typical microstructures are bainite, tempered bainite, tempered martensite, and ferrite and pearlite. All ferritic steels have body centered cubic crystal structures that display ductile-to-cleavage transition temperature fracture toughness characteristics. See also Test Methods E23, E208 and E436.

NOTE 1—This definition is not intended to imply that all of the many possible types of ferritic steels have been verified as being amenable to analysis by this test method.

3.2.2 *stress-intensity factor,  $K[FL^{-3/2}]$* —the magnitude of the mathematically ideal crack-tip stress field coefficient (stress field singularity) for a particular mode of crack-tip region deformation in a homogeneous body.

<sup>3</sup> For referenced ASTM standards, visit the ASTM website, www.astm.org, or contact ASTM Customer Service at service@astm.org. For *Annual Book of ASTM Standards* volume information, refer to the standard's Document Summary page on the ASTM website.

### 3.2.3 Discussion—

In this test method, Mode I is assumed. See Terminology E1823 for further discussion.

3.2.4 *J-integral,  $J[FL^{-1}]$* —a mathematical expression; a line or surface integral that encloses the crack front from one crack surface to the other; used to characterize the local stress-strain field around the crack front (9). See Terminology E1823 for further discussion.

### 3.3 Definitions of Terms Specific to This Standard:

3.3.1 *control force,  $P_m[F]$* —a calculated value of maximum force, used in 7.8.1 to stipulate allowable precracking limits.

3.3.2 *crack initiation*—describes the onset of crack propagation from a preexisting macroscopic crack created in the specimen by a stipulated procedure.

3.3.3 *effective modulus,  $E_{eff}[FL^{-2}]$* —an elastic modulus that allows a theoretical (modulus normalized) compliance to match an experimentally measured compliance for an actual initial crack size,  $a_o$ .

3.3.4 *effective yield strength,  $\sigma_Y[FL^{-2}]$* , — an assumed value of uniaxial yield strength that represents the influence of plastic yielding upon fracture test parameters.

### 3.3.4.1 Discussion—

It is calculated as the average of the 0.2 % offset yield strength  $\sigma_{YS}$ , and the ultimate tensile strength,  $\sigma_{TS}$  as follows:

$$\sigma_Y = \frac{(\sigma_{YS} + \sigma_{TS})}{2}$$

3.3.5 *elastic modulus,  $E$  [ $FL^{-2}$ ]*—a linear-elastic factor relating stress to strain, the value of which is dependent on the degree of constraint. For plane stress,  $E' = E$  is used, and for plane strain,  $E/(1 - \nu^2)$  is used, with  $E$  being Young's modulus and  $\nu$  being Poisson's ratio.

3.3.6 *elastic plastic  $J_c$  [ $FL^{-1}$ ]*— $J$ -integral at the onset of cleavage fracture.

3.3.7 *elastic-plastic  $K_J$  [ $FL^{-3/2}$ ]*—An elastic-plastic equivalent stress intensity factor derived from the  $J$ -integral.

### 3.3.7.1 Discussion—

In this test method,  $K_J$  also implies a stress intensity factor determined at the test termination point under conditions determined to be invalid by 8.9.2.

3.3.8 *elastic-plastic  $K_{Jc}$  [ $FL^{-3/2}$ ]*—an elastic-plastic equivalent stress intensity factor derived from the  $J$ -integral at the point of onset of cleavage fracture,  $J_c$ .

3.3.9 *equivalent value of median toughness,  $K_{Jc}^{eq}$  [ $FL^{-3/2}$ ]*—an equivalent value of the median toughness for a multi-temperature data set.

3.3.10 *Eta ( $\eta$ )*—a dimensionless parameter that relates plastic work done on a specimen to crack growth resistance defined in terms of deformation theory  $J$ -integral (10).

3.3.11 *failure probability,  $p_f$* —the probability that a single selected specimen chosen at random from a population of specimens will fail at or before reaching the  $K_{Jc}$  value of interest.

3.3.12 *initial ligament length,  $b_o$  [ $L$ ]*—the distance from the initial crack tip,  $a_o$ , to the back face of a specimen.

3.3.13 *load-line displacement rate,  $\dot{\Delta}_{LL}$  [ $LT^{-1}$ ]*—rate of increase of specimen load-line displacement.

3.3.14 *pop-in*—a discontinuity in a force versus displacement test record (11).

### 3.3.14.1 Discussion—

#### ASTM E1921-14a

A pop-in event is usually audible, and is a sudden cleavage crack initiation event followed by crack arrest. A test record will show increased displacement and drop in applied force if the test frame is stiff. Subsequently, the test record may continue on to higher forces and increased displacement.

3.3.15 *precracked Charpy, PCC, specimen*—SE(B) specimen with  $W = B = 10$  mm (0.394 in.).

3.3.16 *provisional reference temperature, ( $T_{oQ}$ ) [ $^{\circ}C$ ]*—Interim  $T_o$  value calculated using the standard test method described herein. If all validity criteria are met then  $T_o = T_{oQ}$ .

3.3.17 *reference temperature,  $T_o$  [ $^{\circ}C$ ]*—The test temperature at which the median of the  $K_{Jc}$  distribution from 1T size specimens will equal 100 MPa $\sqrt{m}$  (91.0 ksi $\sqrt{in.}$ ).

3.3.18 *SE(B) specimen span,  $S$  [ $L$ ]*—the distance between specimen supports (See Test Method E1820 Fig. 3).

3.3.19 *specimen thickness,  $B$  [ $L$ ]*—the distance between the parallel sides of a test specimen as depicted in Figs. 1-3.

### 3.3.19.1 Discussion—

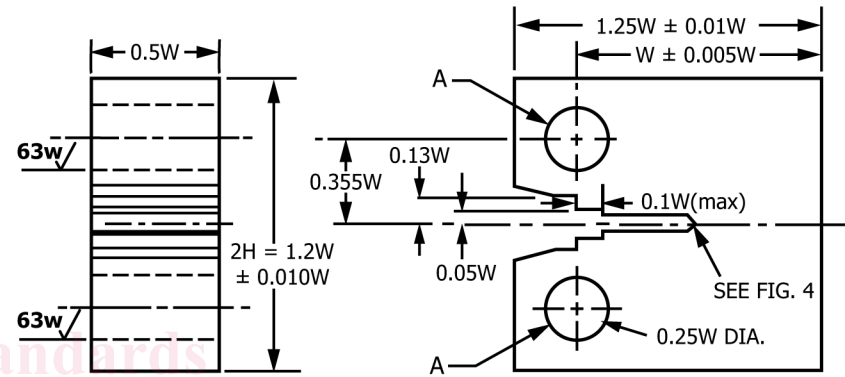
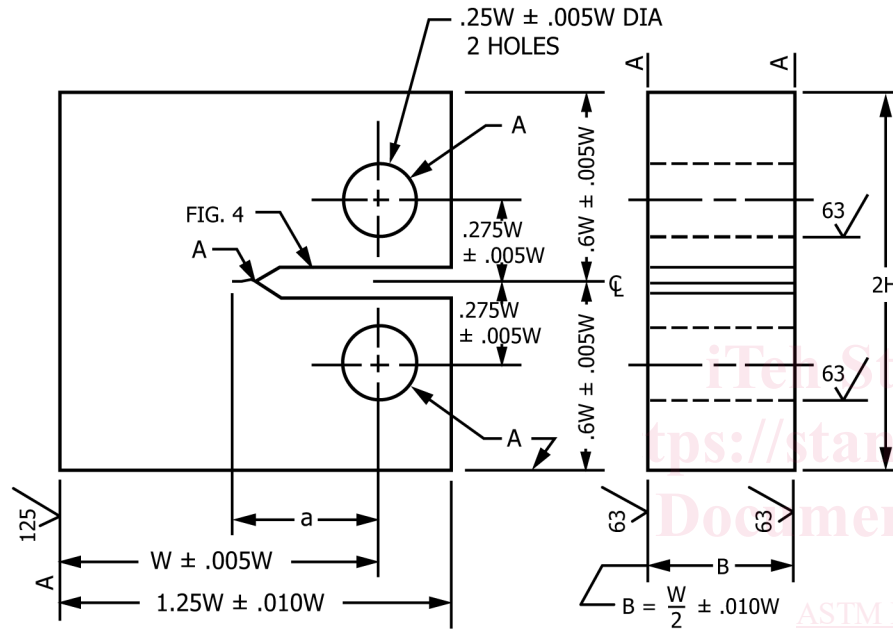
In the case of side-grooved specimens, the net thickness,  $B_N$ , is the distance between the roots of the side-groove notches.

3.3.20 *specimen size,  $nT$* —a code used to define specimen dimensions, where  $n$  is expressed in multiples of 1 in.

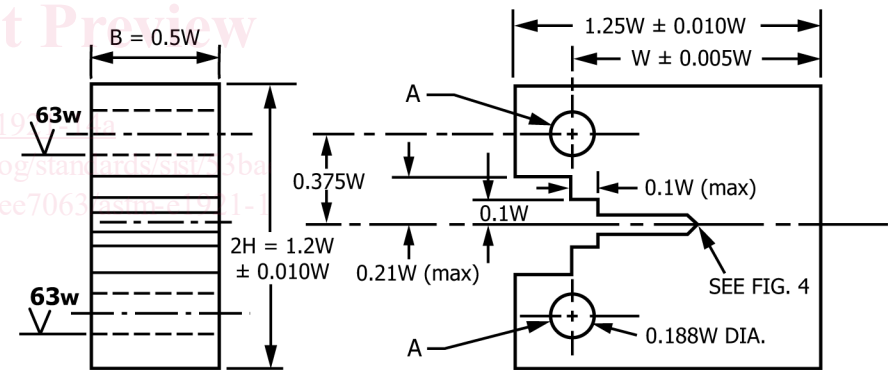
### 3.3.20.1 Discussion—

In this method, specimen proportionality is required. For compact specimens and bend bars, specimen thickness  $B = n$  inches.

3.3.21 *temperature,  $T_{oX}^{est}$  [ $^{\circ}C$ ]*—estimated value of the reference temperature corresponding to an elevated loading rate X, to be used only for test temperature selection in accordance with 8.4.2.



COMPACT TEST SPECIMEN FOR PIN OF 0.24W (+0.000W/-0.005W) DIAMETER

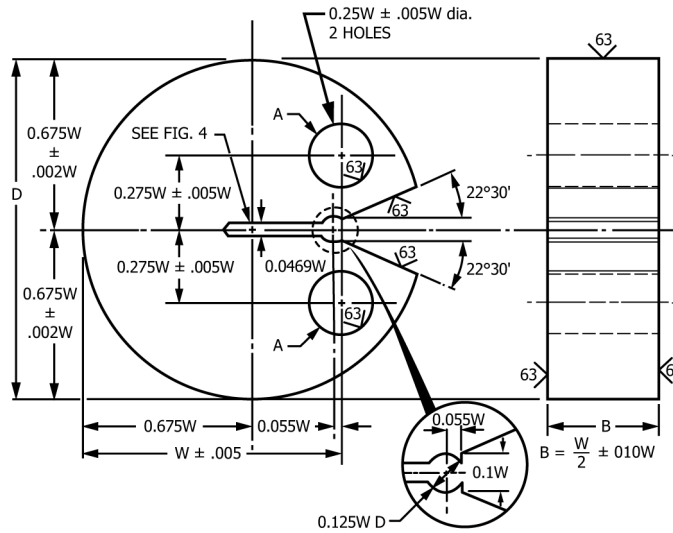


COMPACT TEST SPECIMEN FOR PIN OF 0.1875W (+0.000W/ - 0.001W) DIAMETER

NOTE 1—"A" surfaces shall be perpendicular and parallel as applicable to within 0.002W TIR.

NOTE 2—The intersection of the crack starter notch tips with the two specimen surfaces shall be equally distant from the top and bottom edges of the specimen within 0.005W TIR.

FIG. 1 Recommended Compact Specimen Designs

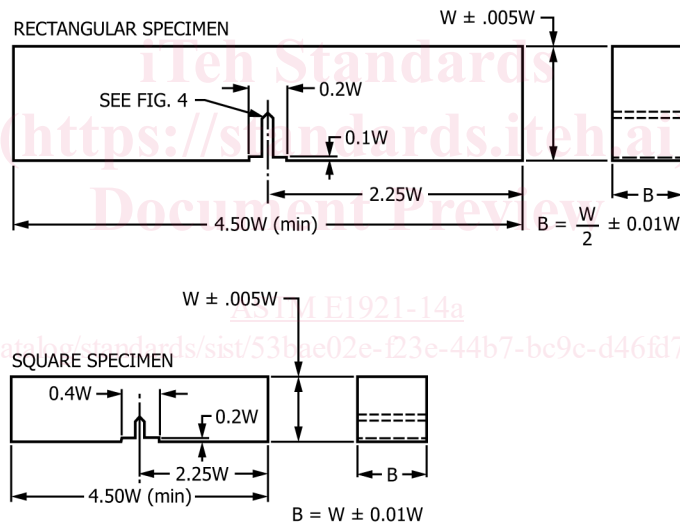


NOTE 1—A surfaces shall be perpendicular and parallel as applicable to within 0.002W TIR.

NOTE 2—The intersection of the crack starter notch tips with the two specimen surfaces shall be equally distant from the top and bottom extremes of the disk within 0.005W TIR.

NOTE 3—Integral or attached knife edges for clip gage attachment may be used. See also Fig. 6, Test Method E399.

FIG. 2 Disk-shaped Compact Specimen DC(T) Standard Proportions



NOTE 1—All surfaces shall be perpendicular and parallel within 0.001W TIR; surface finish 64v.

NOTE 2—Crack starter notch shall be perpendicular to specimen surfaces to within  $\pm 2^\circ$ .

FIG. 3 Recommended Bend Bar Specimen Design

3.3.22 *temperature,  $T_Q$  [ $^\circ\text{C}$ ]*—For  $K_{Jc}$  values that are developed using specimens or test practices, or both, that do not conform to the requirements of this test method, a temperature at which  $K_{Jc}(\text{med}) = 100 \text{ MPa}\sqrt{\text{m}}$  is defined as  $T_Q$ .  $T_Q$  is not a provisional value of  $T_o$ .

3.3.23 *test loading rate  $K$  [ $\text{FL}^{-3/2}\text{T}^{-1}$ ]*—rate of increase of applied stress intensity factor.

3.3.23.1 *Discussion*—

It is generally evaluated as the ratio between  $K_{Jc}$  and the corresponding time to cleavage. For tests where partial unloading/reloading sequences are used to measure compliance, an equivalent time to cleavage  $t'_c$  shall be used to calculate the loading rate. The value of  $t'_c$  is calculated as the ratio between the value of load-line displacement at cleavage and the load-line displacement rate applied during the monotonic loading portions of the test (that is, the periods between partial unloading/reloading sequences used for compliance measurement).

3.3.24 *time to control force,  $t_m$  [T]*—time to  $P_m$ .

3.3.25 *Weibull fitting parameter,  $K_0$* —a scale parameter located at the 63.2 % cumulative failure probability level (12).  $K_{Jc} = K_0$  when  $p_f = 0.632$ .

3.3.26 *Weibull slope,  $b$* —with  $p_f$  and  $K_{Jc}$  data pairs plotted in linearized Weibull coordinates obtainable by rearranging Eq 19,  $b$  is the slope of a line that defines the characteristics of the typical scatter of  $K_{Jc}$  data.

#### 3.3.26.1 Discussion—

A Weibull slope of 4 is used exclusively in this method, and in Eq 19.

3.3.27 *yield strength,  $\sigma_{YS}$  [ $FL^{-2}$ ]*—the stress at which a material exhibits a specific limiting deviation from the proportionality of stress to strain at the test temperature. This deviation is expressed in terms of strain.

#### 3.3.27.1 Discussion—

1 It is customary to determine yield strength by either (1) Offset Method (usually a strain of 0.2 % is specified) or (2) Total-Extension-Under-Force Method (usually a strain of 0.5 % is specified although other values of strain may be used).

#### 3.3.27.2 Discussion—

2 Whenever yield strength is specified, the method of test must be stated along with the percent offset or total strain under force. The values obtained by the two methods may differ.

## 4. Summary of Test Method

4.1 This test method involves the testing of notched and fatigue precracked bend or compact specimens in a temperature range where either cleavage cracking or crack pop-in develop during the loading of specimens. Crack aspect ratio,  $a/W$ , is nominally 0.5. Specimen width in compact specimens is two times the thickness. In bend bars, specimen width can be either one or two times the thickness.

4.2 Force versus displacement across the notch at a specified location is recorded by autographic recorder or computer data acquisition, or both. Fracture toughness is calculated at a defined condition of crack instability. The  $J$ -integral value at instability,  $J_c$ , is calculated and converted into its equivalent in units of stress intensity factor,  $K_{Jc}$ . Validity limits are set on the suitability of data for statistical analyses.

4.3 ~~Tests that are replicated at least six times can be~~ Valid data sets are used to estimate the median  $K_{Jc}$  of the Weibull distribution for the data population (13). Extensive data scatter among replicate tests is expected. Statistical methods are used to characterize these data populations and to predict changes in data distributions with changed specimen size.

4.4 The statistical relationship between specimen size and  $K_{Jc}$  fracture toughness ~~can be~~ is assessed using weakest-link theory, thereby providing a relationship between the specimen size and  $K_{Jc}$  (4). Limits are placed on the fracture toughness range over which this model can be used.

4.5 For definition of the toughness transition curve, a master curve concept is used (14, 15). The position of the curve on the temperature coordinate is established from the experimental determination of the temperature, designated  $T_o$ , at which the median  $K_{Jc}$  for 1T size specimens is 100 MPa $\sqrt{m}$  (91.0 ksi $\sqrt{in.}$ ). Selection of a test temperature close to that at which the median  $K_{Jc}$  value will be 100 MPa $\sqrt{m}$  is encouraged and a means of estimating this temperature is suggested. Small specimens such as precracked Charpy's may have to be tested at temperatures below  $T_o$  where  $K_{Jc(med)}$  is well below 100 MPa $\sqrt{m}$ . In such cases, additional specimens may be required as stipulated in 8.5.

4.6 Tolerance bounds can be determined that define the range of scatter in fracture toughness throughout the transition range. The standard deviation of the fitted distribution is a function of Weibull slope and median  $K_{Jc}$  value,  $K_{Jc(med)}$ .

## 5. Significance and Use

5.1 Fracture toughness is expressed in terms of an elastic-plastic stress intensity factor,  $K_{Jc}$ , that is derived from the  $J$ -integral calculated at fracture.

5.2 Ferritic steels are microscopically inhomogeneous with respect to the orientation of individual grains. Also, grain boundaries have properties distinct from those of the grains. Both contain carbides or nonmetallic inclusions that can act as nucleation sites for cleavage microcracks. The random location of such nucleation sites with respect to the position of the crack front manifests itself as variability of the associated fracture toughness (16). This results in a distribution of fracture toughness values that is amenable to characterization using the statistical methods in this test method.

5.3 The statistical methods in this test method presume that the test materials are macroscopically homogeneous such that both the tensile and toughness properties are uniform. The fracture toughness evaluation of nonuniform materials is not amenable to

the statistical analysis methods employed in the main body of this test method. For example, multipass weldments can create heat-affected and brittle zones with localized properties that are quite different from either the bulk material or weld. Thick section steel also often exhibits some variation in properties near the surfaces. An appendix to analyze the cleavage toughness properties of nonuniform or inhomogeneous materials is currently being prepared. In the interim, users are referred to (6-8) for procedures to analyze inhomogeneous materials. Metallographic analysis can be used to identify possible nonuniform regions in a material. These regions can then be evaluated through mechanical testing such as hardness, microhardness, and tensile testing to compare with the bulk material. It is also advisable to measure the toughness properties of these nonuniform regions distinctly from the bulk material.

5.4 Distributions of  $K_{Jc}$  data from replicate tests can be used to predict distributions of  $K_{Jc}$  for different specimen sizes. Theoretical reasoning (12), confirmed by experimental data, suggests that a fixed Weibull slope of 4 applies to all data distributions and, as a consequence, standard deviation on data scatter can be calculated. Data distribution and specimen size effects are characterized using a Weibull function that is coupled with weakest-link statistics (17). An upper limit on constraint loss and a lower limit on test temperature are defined between which weakest-link statistics can be used.

5.5 The experimental results can be used to define a master curve that describes the shape and location of median  $K_{Jc}$  transition temperature fracture toughness for 1T specimens (18). The curve is positioned on the abscissa (temperature coordinate) by an experimentally determined reference temperature,  $T_o$ . Shifts in reference temperature are a measure of transition temperature change caused, for example, by metallurgical damage mechanisms.

5.6 Tolerance bounds on  $K_{Jc}$  can be calculated based on theory and generic data. For added conservatism, an offset can be added to tolerance bounds to cover the uncertainty associated with estimating the reference temperature,  $T_o$ , from a relatively small data set. From this it is possible to apply a margin adjustment to  $T_o$  in the form of a reference temperature shift.

5.7 For some materials, particularly those with low strain hardening, the value of  $T_o$  may be influenced by specimen size due to a partial loss of crack-tip constraint (5). When this occurs, the value of  $T_o$  may be lower than the value that would be obtained from a data set of  $K_{Jc}$  values derived using larger specimens.

5.8 As discussed in 1.3, there is an expected bias among  $T_o$  values as a function of the standard specimen type. The magnitude of the bias may increase inversely to the strain hardening ability of the test material at a given yield strength, as the average crack-tip constraint of the data set decreases (19). On average,  $T_o$  values obtained from C(T) specimens are higher than  $T_o$  values obtained from SE(B) specimens. Best estimate comparison indicates that the average difference between C(T) and SE(B)-derived  $T_o$  values is approximately 10 °C (2). However, individual C(T) and SE(B) datasets may show much larger  $T_o$  differences (3, 20, 21), or the SE(B)  $T_o$  values may be higher than the C(T) values (2). On the other hand, comparisons of individual, small datasets may not necessarily reveal this average trend. Datasets which contain both C(T) and SE(B) specimens may generate  $T_o$  results which fall between the  $T_o$  values calculated using solely C(T) or SE(B) specimens.

## 6. Apparatus

6.1 *Precision of Instrumentation*—Measurements of applied forces and load-line displacements are needed to obtain work done on the specimen. Force versus load-line displacements ~~may~~shall be recorded digitally on computers or autographically on  $x$ - $y$  plotters. For computers, digital signal resolution ~~should~~shall be at least 1/32,000 of the displacement transducer signal range and shall be at least 1/4,000 of the force transducer signal range.

6.2 *Grips for C(T) Specimens*—A clevis with flat-bottom holes is recommended. See Test Method E399, Fig. A6.2, for a recommended design. Clevises and pins should be fabricated from steels of sufficient strength to elastically resist indentation loads (greater than 40 Rockwell hardness C scale (HRC)).

6.3 *Bend Test Fixture*—A suitable bend test fixture scheme is shown in Fig. A3.2 of Test Method E399. It allows for roller pin rotation and minimizes friction effects during the test. Fixturing and rolls should be made of high-hardness steel (HRC greater than 40).

### 6.4 *Displacement Gage for Compact Specimens:*

6.4.1 Displacement measurements are made so that  $J$  values ~~can be~~are determined from area under force versus displacement test records (a measure of work done). If the test temperature selection recommendations of this practice are followed, crack growth measurement will probably prove to be unimportant. Results that fall within the limits of uncertainty of the recommended test temperature estimation scheme will probably not have significant slow-stable crack growth prior to instability. Nevertheless, crack growth measurements are recommended to provide supplementary information, and these results may be reported.

6.4.2 Unloading compliance is the primary recommendation for measuring slow-stable crack growth. See Test Method E1820. When multiple tests are performed sequentially at low test temperatures, there will be condensation and ice buildup on the grips between the loading pins and flats of the clevis holes. Ice will interfere with the accuracy of the unloading compliance method. Alternatively, crack growth can be measured by other methods such as electric potential, but care must be taken to avoid specimen heating when low test temperatures are used.

6.4.3 In compact C(T) specimens, displacement measurements on the load-line are recommended for  $J$  determinations. However, the front face position at  $0.25W$  in front of the load-line can be used with interpolation to load-line displacement, as suggested in 7.1.

6.4.4 The extensometer calibrator shall be resettable at each displacement interval within 0.0051 mm (0.0002 in.). Accuracy of the clip gage at test temperature must be demonstrated to be within 1 % of the working range of the gage.

6.4.5 All clip gages used shall have temperature compensation.

#### 6.5 Displacement Gages for Bend Bars, SE(B):

6.5.1 The SE(B) specimen has two displacement gage locations. A load-line displacement transducer is primarily intended for  $J$  computation, but may also be used for calculations of crack size based on elastic compliance, if provision is made to subtract the extra displacement due to the elastic compliance of the fixturing. The load-line gage shall display accuracy of 1 % over the working range of the gage. The gages used shall not be temperature sensitive.

6.5.2 Alternatively, a crack-mouth opening displacement (CMOD) gage can also be used to determine the plastic part of  $J$ . However, it is necessary to employ a plastic eta ( $\eta$ ) value developed specifically for the CMOD location (22) or infer load-point displacement from CMOD using an expression that relates the two displacements (23). In either case, the procedure described in 9.1.4 is used to calculate the plastic part of  $J$ . However, it is recommended that the plastic part of  $J$  be estimated from the direct CMOD or load-line displacement measurement rather than inferring load-line displacement from CMOD. Additionally, CMOD measurement is more accurate than load-line displacement for estimating crack length from compliance.

6.5.3 Crack growth can be measured by alternative methods such as electric potential, but care must be taken to minimize specimen heating effects in low-temperature tests (see also 6.4.2) (24).

#### 6.6 Force Measurement:

6.6.1 Testing shall be performed in a machine conforming to Practices of E4 and Test Methods E8/E8M. Applied force may be measured by any transducer with a noise-to-signal ratio less than 1/2,000 of the transducer signal range.

6.6.2 Calibrate force measurement instruments by way of Practice E74, 10.2. Annual calibration using calibration equipment traceable to the National Institute of Standards and Technology is a mandatory requirement.

6.7 Temperature Control—Specimen temperature shall be measured with thermocouple wires and potentiometers. It is recommended that the two thermocouple wires be attached to the specimen surface separately, either by welding, spot welding, or by being affixed mechanically. Mechanical attachment schemes must be verified to provide equivalent temperature measurement accuracy. The purpose is to use the test material as a part of the thermocouple circuit (see also 8.6.1). Accuracy of temperature measurement shall be within 3°C of true temperature and repeatability among specimens shall be within 2°C. Precision of measurement shall be  $\pm 1^\circ\text{C}$  or better. The temperature measuring apparatus shall be checked every six months using instruments traceable to the National Institute of Standards and Technology in order to ensure the required accuracy.

## 7. Specimen Configuration, Dimensions, and Preparation

7.1 Compact Specimens—Three recommended C(T) specimen designs are shown in Fig. 1. One C(T) specimen configuration is taken from Test Method E399; the two with cutout sections are taken from E1820. The latter two designs are modified to permit load-line displacement measurement. Room is provided for attachment of razor blade tips on the load-line. Care should be taken to maintain parallel alignment of the blade edges. When front face (at  $0.25W$  in front of the load-line) displacement measurements are made with the Test Method E399 design, the load-line displacement can be inferred by multiplying the measured values by the constant 0.73 (25). The ratio of specimen height to width,  $2H/W$  is 1.2, and this ratio is to be the same for all types and sizes of C(T) specimens. The initial crack size,  $a_o$ , shall be  $0.5W \pm 0.05W$ . Specimen width,  $W$ , shall be  $2B$ .

7.2 Disk-shaped Compact Specimens—A recommended DC(T) specimen design is shown in Fig. 2. Initial crack size,  $a_o$ , shall be  $0.5W \pm 0.05W$ . Specimen width shall be  $2B$ .

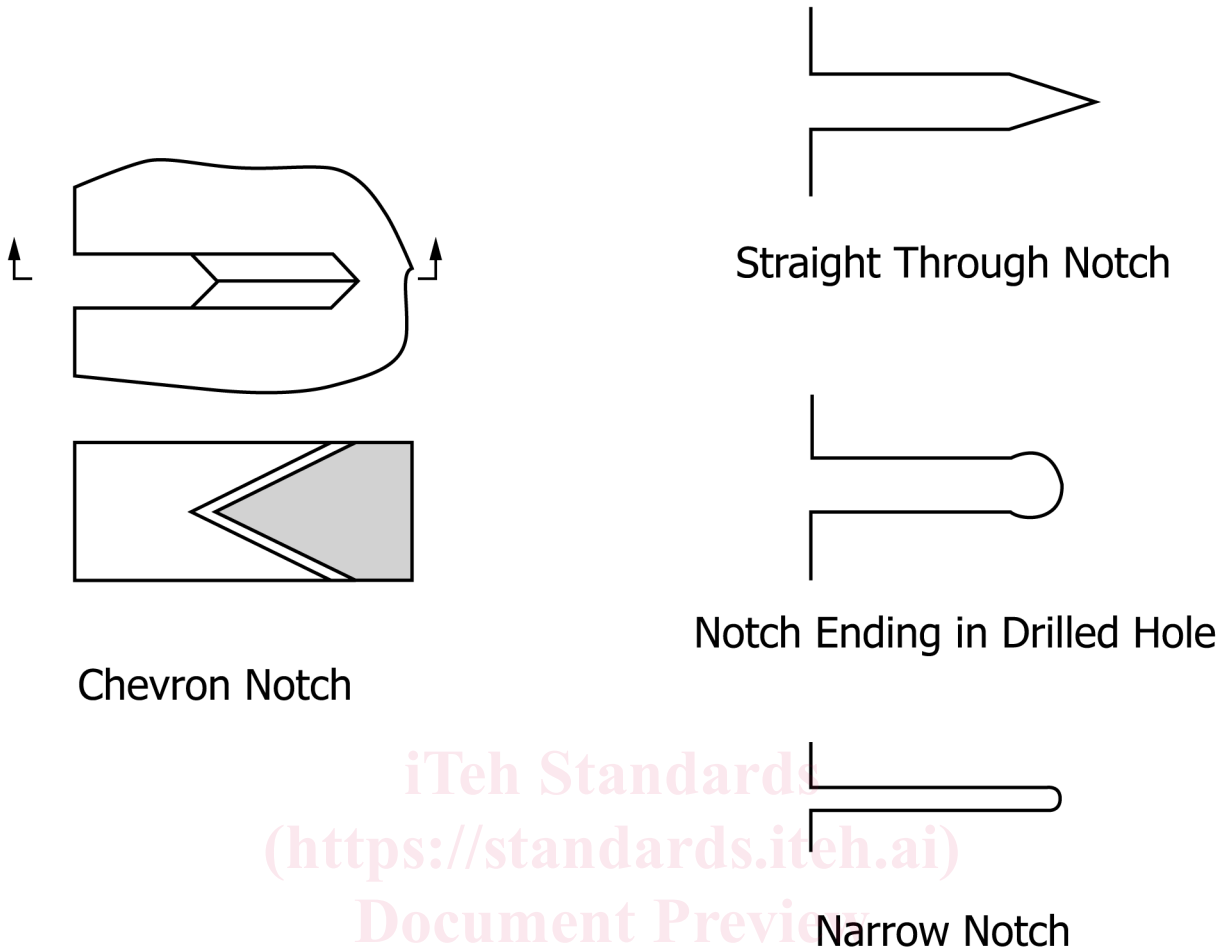
7.3 Single-edge Notched Bend—The recommended SE(B) specimen designs, shown in Fig. 3, are made for use with a span-to-width ratio,  $S/W = 4$ . The width,  $W$ , can be either  $1B$  or  $2B$ . The initial crack size,  $a_o$ , shall be  $0.5W \pm 0.05W$ .

7.4 Machined Notch Design—Three designs of fatigue crack starter notches are shown in Fig. 4. These notches can be straight through the specimen thickness or incorporate the chevron form (Fig. 4). The machined notch plus fatigue crack for all specimens shall lie within the envelope shown in Fig. 5. To facilitate fatigue cracking at low stress intensity levels, the root radius for a straight-through slot terminating in a V-notch should be 0.08 mm (0.003 in.) or less. If a chevron form of notch is used, the root radius may be 0.25 mm (0.010 in.) or less. In the case of a notch ending in a drilled hole, it will be necessary to provide a sharp stress raiser at the end of the hole.

7.5 Specimen Dimension Requirements—The crack front straightness criterion defined in 8.9.1 must be satisfied. The specimen remaining ligament,  $b_o$ , must have sufficient size to maintain a condition of high crack-front constraint at fracture. The maximum  $K_{Jc}$  capacity of a specimen is given by:

$$K_{Jc(\text{limit})} = \sqrt{\frac{Eb_o\sigma_{YS}}{30(1-\nu^2)}} \quad (1)$$





NOTE 1—Notch width need not be less than 1.6mm (1/16 in.) but not exceed 0.063W.

NOTE 2—The intersection of the crack starter surfaces with the two specimen faces shall be equidistant from the top and bottom edges of the specimen within 0.005W.

FIG. 4 Envelope Crack Starter Notches

where:

$$b_o = W - a_o$$

$K_{Jc}$  data that exceed this requirement may be used in a data censoring procedure. Details of this procedure are described in 10.2.1.

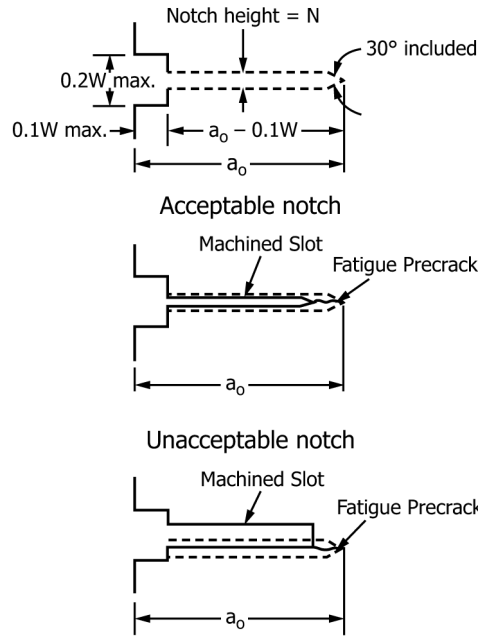
7.6 *Small Specimens*—At high values of fracture toughness relative to specimen size and material flow properties, the values of  $K_{Jc}$  that meet the requirements of Eq 1 may not always provide a unique description of the crack-front stress-strain fields due to some loss of constraint caused by excessive plastic flow (5). This condition may develop in materials with low strain hardening. When this occurs, the highest  $K_{Jc}$  values of the valid data set could possibly cause the value of  $T_o$  to be lower than the value that would be obtained from testing specimens with higher constraint.

7.7 *Side Grooves*—Side grooves are optional. Precracking prior to side-grooving is recommended, despite the fact that crack growth on the surfaces might be slightly behind. Specimens may be side-grooved after precracking to decrease the curvature of the initial crack front. In fact, side-grooving may be indispensable as a means for controlling crack front straightness in bend bars of square cross section. The total side-grooved depth shall not exceed 0.25B. Side grooves with an included angle of 45° and a root radius of 0.5 ± 0.2 mm (0.02 ± 0.01 in.) usually produce the desired results.

7.8 *Precracking:*

7.8.1 *Fatigue Loading Requirements*—Allowable fatigue force values are limited to keep the maximum stress intensity factor applied during precracking,  $K_{max}$ , well below the material fracture toughness measured during the subsequent test. The fatigue precracking shall be conducted with the specimen fully heat-treated to the condition in which it is to be tested. No intermediate heat treatments between precracking and testing are allowed. The combination of starter notch and fatigue precrack shall conform to the requirements shown in Fig. 5. There are several ways of promoting early crack initiation: (1) by providing a very sharp notch tip, (2) by using a chevron notch (Fig. 4), (3) by statically preloading the specimen in such a way that the notch tip is compressed

Notch and required crack envelope



Notch and Precrack Configurations

	Wide Notch	Narrow Notch
Maximum Notch Height	Lesser of 0.063W or 6.25 mm	0.01W
Maximum Notch Angle	60°	As machined
Minimum Precrack Length	Greater of 0.5N or 1.3 mm	Greater of 0.5N or 0.6mm

NOTE 1—The crack-starter notch shall be centered between the top and bottom specimen edges within 0.005W.

FIG. 5 Envelope of Fatigue Crack and Crack Starter Notches

in a direction normal to the intended crack plane (to a force not to exceed  $P_m$ ), and (4) by using a negative fatigue force ratio; for a given maximum fatigue force, the more negative the force ratio, the earlier crack initiation is likely to occur. The peak compressive force shall not exceed  $P_m$  as defined in the equations below:

$$\text{For SE(B) specimens, } P_m = \frac{0.5Bb_o^2\sigma_Y}{S} \quad (2)$$

$$\text{For C(T) and DC(T) specimens, } P_m = \frac{0.4Bb_o^2\sigma_Y}{2W+a_o} \quad (3)$$

**7.8.2 Fatigue Precracking Procedure**—Fatigue precracking can be conducted under either force control, displacement control, or  $K$  control. If the force cycle is maintained constant, the maximum  $K$  and  $\Delta K$  will increase with crack size; if the displacement cycle is maintained constant, the reverse will happen. If  $K$  is maintained constant, force has to be reduced as a function of increasing crack size. Fatigue cycling is conducted using a sinusoidal waveform and a frequency close to the highest practical value. There is no known marked frequency effect on fatigue precrack formation up to at least 100 Hz in the absence of adverse environments. The specimen shall be accurately located in the loading fixture to achieve uniform, symmetric loading. The specimen should be carefully monitored until crack initiation is observed on one side. If crack initiation is not observed on the other side before appreciable growth is observed on the first side, then fatigue cycling should be stopped to try to determine the cause and find a remedy for the unsymmetrical behavior. Sometimes, simply turning the specimen around in relation to the fixture will solve the problem.

Precracking can be performed either by some method of smoothly and continually decreasing the maximum stress intensity factor ( $K_{max}$ ) or by using discrete steps. It is suggested that the reduction in  $K_{max}$  between any discrete step be no greater than 20% because reducing  $K_{max}$  too rapidly can result in precrack growth rate retardation. It is also suggested that measurable crack extension occur before proceeding to the next step. Precracking is generally most effectively conducted using  $R = P_{min}/P_{max} = 0.1$ . Maximum force values shall be accurate to within  $\pm 5\%$  of their target values.

Fig. 6 shows the allowable envelope for  $K_{max}$  during precracking. The precracking  $K_{max}$  and crack extension requirements are summarized in Table 1, and Table 2. Precracking can be conducted in any manner such that  $K_{max}$  remains within the envelope and the maximum fatigue force is less than  $P_m$ . The  $K_{max}$  applied to the specimen shall not exceed 25 MPa√m (22.8 ksi√in) at any crack length, and may be limited by  $P_m$  for small specimens or low yield strength materials, or both. As the testing temperature decreases

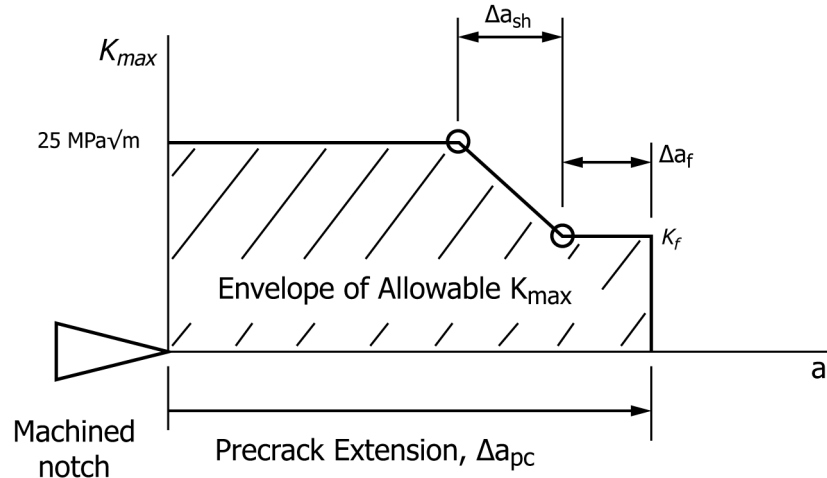


FIG. 6 Envelope of Allowable  $K_{max}$  During Precracking

TABLE 1  $K_{max}$  Requirements

Initial:  $K_{max}$  cannot exceed 25 MPa√m (22.8 ksi√in.) and the maximum fatigue force cannot exceed  $P_m$ .

Final:  $K_f$  depends on the test temperature:

Test Temperature	$K_f$ throughout $\Delta a_f$
< precracking temperature	< 15 MPa√m (13.7 ksi√in.)
≥ precracking temperature	< 20 MPa√m (18.3 ksi√in.)

TABLE 2 Crack Extension Requirements

Wide Notch ( $N \geq 0.01W$ )	$\Delta a_{min} = 1.3\text{mm (0.050 in.)}$
Narrow Notch ( $N < 0.01W$ )	$\Delta a_{min} = 0.6\text{ mm (0.024 in.)}$

$$\Delta a_{pc} \geq 0.5N \text{ and } \Delta a_{min}$$

$$\Delta a_{sh} \geq r_{p1} - r_{p2}$$

ASTM E1921

Where: <https://standards.iteh.ai/catalog/standards/sist/53bae02e-f23e-44b7-be9c-d46fd7ee7063/astm-e1921-14a>

$$r_{p1} = \frac{1}{3\pi} \left( \frac{K_{max}}{\sigma_{ys}} \right)^2 \text{ with } K_{max}$$

$$= 25 \text{ MPa}\sqrt{\text{m (22.8 ksi}\sqrt{\text{in.)}}$$

$$r_{p2} = \frac{1}{3\pi} \left( \frac{K_f}{\sigma_{ys}} \right)^2$$

$$\Delta a_f \geq 0.2 \text{ mm (0.008 in.)}$$

compared to the precracking temperature, the warm prestressing effect increases, which can elevate the measured fracture toughness. To minimize the warm prestressing effect, the maximum  $K$  that may be applied to the specimen during  $\Delta a_f$  ( $K_f$  in Fig. 6) shall not exceed 15 MPa√m (13.7 ksi√in.), where the minimum length of  $\Delta a_f$  (Fig. 6) is 0.2 mm (0.008 in.). Alternatively, when the testing temperature is equal to or above the precracking temperature,  $K_f$  shall not exceed 20 MPa√m (18.3 ksi√in.).  $\Delta a_{sh}$  is greater than or equal to the change in plastic zone size in going from a maximum  $K$  of 25 MPa√m (22.8 ksi√in.) to  $K_f$ . The minimum value for  $\Delta a_{sh}$  defines the condition where the leading edge of the plastic zone remains stationary as  $K_{max}$  is decreased.